
CRYPTONITE: REVEALING THE PITFALLS OF END-TO-END PRIVATE INFERENCE AT SCALE

Karthik Garimella¹ Nandan Kumar Jha¹ Zahra Ghodsi² Siddharth Garg¹ Brandon Reagen¹

ABSTRACT

The privacy concerns of providing deep learning inference as a service have underscored the need for private inference (PI) protocols that protect users’ data and the service provider’s model using cryptographic methods. Recently proposed PI protocols have achieved significant reductions in PI latency by moving the computationally heavy homomorphic encryption (HE) parts to an offline/pre-compute phase. Paired with recent optimizations that tailor networks for PI, these protocols have achieved performance levels that are tantalizingly close to being practical. In this paper, we conduct a rigorous end-to-end characterization of PI protocols and optimization techniques and find that the current understanding of PI performance is overly optimistic. Specifically, we find that offline storage costs of garbled circuits (GC), a key cryptographic protocol used in PI, on user/client devices are prohibitively high and force much of the expensive offline HE computation to the online phase, resulting in a 10-1000 \times increase to PI latency. We propose a modified PI protocol that significantly reduces client-side storage costs for a small increase in online latency. Evaluated end-to-end, the modified protocol outperforms current protocols by reducing the mean PI latency by 4 \times for ResNet18 on TinyImageNet. We conclude with a discussion of several recently proposed PI optimizations in light of the findings and note many actually increase PI latency when evaluated from an end-to-end perspective.

1 INTRODUCTION

Today, privacy continues to increase in relevance as users steadily demand more control over how and when their data is used and collected. Addressing these concerns will likely have a profound effect on how the internet and many popular services, which heavily rely on precise user data for high-quality experiences, are implemented. One popular solution is to leverage privacy-preserving computation techniques that guarantee the privacy and security of user data during computations, thereby extending these guarantees from classical methods that only apply to communication. Privacy-preserving computation provides the best of both worlds for the user: privacy and security are both significantly improved and one still has access to online services integral to everyday life.

The scope of privacy-preserving solutions is vast. Techniques vary in how they achieve security, whether by relying on system implementations (e.g., SGX (Anati et al., 2013), Morpheous (Gallagher et al., 2019)), statistics (e.g. differential privacy (Dwork, 2006; Abadi et al., 2016)), or cryptography (e.g. HE (Rivest et al., 1978; Gentry et al., 2009; Brakerski & Vaikuntanathan, 2011) and multi-party

computation (Shamir, 1979)). Each comes with a trade-off. Relying on systems offers the best performance (e.g., Slalom (Tramer & Boneh, 2018), DarKnight (Hashemi et al., 2021)) but may concede security due to known vulnerabilities (e.g., Foreshadow (Van Bulck et al., 2018)). Statistical privacy is generally much stronger and has the benefit that it can be quantified; for example using ρ (Wood et al., 2018). However, it typically introduces approximation/noise to the computation, which can degrade inference accuracy, and is most applicable to answering questions in aggregate. Therefore, its use in computing on individual user data is still unclear. Cryptography-based solutions provide capabilities to compute exact inferences with very strong security, e.g., 128-bit, but come at the expense of high computational and communication/storage cost. Homomorphic encryption (HE) and secure multi-party computation (MPC) are the two leading methods for cryptographically secure computation.

We explore private inference (PI) using cryptographic primitives in a two-party compute (2PC) setting. In this setting, we assume that a client/user (the first party) has some data they would like to keep private while a server/service provider (the second party) performs inference on the user data using a deep neural network model, which they also want to keep private, on an encrypted representation of the data. We consider only 2PC protocols in this study because they require fewer trust assumptions than other protocols,

¹New York University ²University of California, San Diego.
Correspondence to: Karthik Garimella <kg2383@nyu.edu>.

e.g., trusted third party (TTP), and most closely mirror the plaintext client-server computational setting of today. Our study is motivated by a growing body of work on PI that suggests PI run-times are approaching performance levels necessary for practical deployment. (In contrast, the overheads of private training are farther from practicality. Even so, our PI observations can inform developments in private training also.)

In this paper, we conduct the first end-to-end characterization of PI taking into account realistic system considerations. Current 2PC PI protocols leverage a combination of cryptographic primitives, including HE, secret sharing (SS), garbled circuits (GC), and oblivious transfer (OT). State-of-the-art (SOTA) solutions optimize for online runtime by pre-computing SS constants using HE and preparing GCs in an offline phase, and then evaluating inference inputs using GCs and SS online.

Instances of these protocols, including MiniONN (Liu et al., 2017), Gazelle (Juvekar et al., 2018), CrypTFlow2 (Rathee et al., 2020), DELPHI (Mishra et al., 2020), CryptoNAS (Ghodsi et al., 2020), DeepReDuce (Jha et al., 2021), SAFENets (Lou et al., 2021), etc. (see Table 3 for a comprehensive list) focus only on executing a *single inference* at a time and mainly report improvements for *online* computation/communication latency. This leaves several open questions: (1) who pays for the offline costs, (2) what is the performance over multiple inference requests arriving at different rates, and (3) what is the role of storage cost?

We find that the reported nearly-practical PI latency in recent work can be misleading as the pre-processing times of HE and storage requirements of GCs of each inference are so high that they can only truly be offline at extremely low arrival rates, e.g., 0.001 requests per second. We observe that the standard “Server-Garbler” protocols, as used in DELPHI (Mishra et al., 2020) and Gazelle (Juvekar et al., 2018) CryptoNAS (Ghodsi et al., 2020) and DeepReDuce (Jha et al., 2021), require more than 17KB to store GCs for *each* ReLU in a DNN. Hence, for ResNet-18 on CIFAR-100, roughly 10GB (on TinyImageNet ~40GB) of storage is needed for a *single* inference (See Figure 2c). As a result, clients can only perform a (very) limited number of pre-computation before running out of storage capacity, limiting their ability to utilize the down-time between requests for pre-processing. This is a problem as without sufficient storage to buffer precomputations, the extreme runtime costs of HE must be incurred online, which can reduce online performance by 10-1000 \times . Hence, the offline pre-processing cost is quickly brought online as the system cannot keep up.

Driven by the above analysis, we propose a protocol optimization to overcome the client-device storage limitations by reversing the roles of the client and server during the garbled circuit computation. (We note that this has no im-

pact on security, see Section 3.2 for details.) By reversing the roles of the client and server we enable pre-computed GCs to be stored on the server, which has substantially more storage resources. Using our optimized “Client-Garbler” protocol we find that when assuming a server storage budget of 10 TBs, we can reduce the average PI latency by 4 \times when compared to the standard Server-Garbler protocol on TinyImageNet on ResNet-18.

Finally, we expand our characterization of the optimized protocol to understand how recently proposed PI optimizations, which serve as examples of general design principles for efficient PI, impact performance in end-to-end systems. We find that many papers focusing on ReLU optimization alone may not be sufficient and that some could even degrade performance (see Table 3 for a comprehensive list of prior work). This is because while they can (significantly) reduce the storage pressure on the systems, they do not address extreme HE runtimes, which limit the rate that the offline precomputations can be done to replenish the supply. Thus, we suggest future papers on PI optimization consider optimizing for *both* ReLUs, to limit GC storage cost, and FLOPs, to mitigate high HE runtimes.

We conclude that recent low-latency MPC protocols for PI (including optimizations) are in the end performance limited by HE. When considering arrival rates, or more than one inference in isolation, and practical storage limitations the offline cost quickly overwhelms client/server systems and cause the offline cost to be brought online. HE costs are extreme, e.g., it can take roughly 20 minutes to perform inference on TinyImageNet for ResNet-18, and suggests the need for more work in systems support for HE or looking into secure alternatives for computing secrets.

This paper makes the following contributions:

- We conduct the first systems-level study for state-of-the-art PI techniques. Our experiments using different inference request arrival rates reveal client storage limitations and offline homomorphic encryption times limit performance, even when using optimized MPC protocols for PI.
- To overcome the client-storage limitations, we propose the “Client-Garbler” PI protocol. By switching the roles of parties in existing PI protocols (e.g., as used in DELPHI and Gazelle) we are able to reduce the mean PI latency by 4 \times for ResNet-18 on TinyImageNet.
- Finally, we evaluate recently proposed optimizations for private inference performance, e.g., replacing ReLU with x^2 (Gilad-Bachrach et al., 2016; Mishra et al., 2020) and ReLU dropping (Jha et al., 2021). We find that when considering end-to-end system-level effects many optimizations offer limited benefit. Our

analysis motivates the need for more research into reducing both ReLU and FLOP costs in DNN models.

2 PRELIMINARIES

In this section, we provide a brief summary of the cryptographic building blocks used for privacy-preserving inference and show how they can be combined to construct an end-to-end protocol.

2.1 Cryptographic Primitives

Additive Secret Sharing. Additive secret sharing (SS) is a protocol that allows a value x to be split amongst two (or more) parties such that neither party learns anything about x from its share while the two parties can reconstruct x if they work together.

Specifically, the shares of a value x are $\langle x \rangle_1 = r$ and $\langle x \rangle_2 = x - r$, where r is a random value and the arithmetic operations are module a prime p . Since $x = \langle x \rangle_1 + \langle x \rangle_2$, the value x can be recovered if the two parties add their shares together. However, since r is random, neither party has enough information to reconstruct x by itself.

Given shares of two values x and y , shares of $x + y$ can be computed by as follows: $\langle x + y \rangle_1 = \langle x \rangle_1 + \langle y \rangle_1$, and $\langle x + y \rangle_2 = \langle x \rangle_2 + \langle y \rangle_2$. That is, the shares of a sum of two values equal the sum of the shares.

Homomorphic Encryption. HE is a cryptographic protocol that allows a client to encrypt its data in a manner that allows a server to compute a function on the client’s data without ever decrypting the data. HE involves three steps. First, the client encrypts data x using encryption function E and its public key k_{pub} , i.e., $c = E(x, k_{pub})$ (or just $c = E(x)$ for short). Then, given two cipher-texts $c_1 = E(x_1)$ and $c_2 = E(x_2)$, the server homomorphically computes $x_1 \odot x_2$ using a function \star that operates directly on ciphertexts, i.e., $c' = c_1 \star c_2$. The client can then decrypt c' using decryption function D and secret key k_{sec} to obtain $x_1 \odot x_2 = D(c', k_{sec})$ (or just $D(c')$ for short). We will also write $c_1 \star c_2$ as $HE(x_1 \odot x_2)$ for clarity.

Oblivious Transfer. OT (Rabin, 2005) is a fundamental building block in MPC and the foundation for many constructions. In 1-out-2 OT there are two parties: the sender and the receiver. The sender has two input values x_0, x_1 , and the receiver takes as input only a selection bit r . The OT protocol allows the receiver to obtain one of the sender’s inputs corresponding to their selection bit (x_r). The sender will not learn any information, and the receiver will not learn the other input value (x_{1-r}). Although OT protocols require expensive public-key cryptography, it is possible to use a small number of *base OTs* and extend them to achieve a larger number of OTs using cheaper symmetric key cryp-

tography operations (Ishai et al., 2003). These are referred to as *OT extensions*.

Garbled Circuits. The GC protocol was first introduced by Yao (Yao, 1986) and it enables two parties to compute a Boolean function on their private inputs without revealing their inputs to each other. The function is first represented as a Boolean circuit, and one party (the garbler) assigns two random labels (keys) to each wire of the circuit, corresponding to values 0 and 1. For each gate, the garbler then generates an encrypted truth table that maps the output labels to the gate’s input labels. The garbler sends the generated garbled circuit to the other party (the evaluator), along with the labels corresponding to its inputs. The evaluator then uses the OT protocol to obtain the labels corresponding to its inputs without the garbler learning the input values. At this point, the evaluator can execute the circuit gate by gate, without learning intermediate values. Finally, the evaluator shares the output labels with the garbler who maps them to plaintext values.

2.2 Protocol for Private Inference

We begin by reviewing a class of PI protocols that use HE and SS for linear layers, and GCs for ReLU layers (Liu et al., 2017; Juvekar et al., 2018; Mishra et al., 2020). These protocols have achieved SOTA results in the 2PC setting. In this setting, we assume a client and a server who wish to obtain the server’s model prediction on the client’s input while preserving the privacy of both the model and the input. Following prior work, we assume both parties are honest-but-curious, i.e., they follow the protocol faithfully but try to extract information during protocol execution.

We provide a brief description of the DELPHI protocol below, with a depiction in Figure 1(a). The protocol consists of an offline phase, which only depends on the network architecture and parameters, and an online phase, which is performed after the client’s input is available. We represent model parameters at layer i with \mathbf{W}_i (omitting biases in the description for simplicity). The layers after each linear and ReLU operation are represented by \mathbf{x}_i and \mathbf{y}_i , respectively. At a high level, the protocol allows the client and the server to hold additive shares of each layer value during inference evaluation. We assume DELPHI as a baseline (Server-Garbler) protocol in this paper.

Offline Phase. During the offline phase, the client generates the encryption keys and sends them to the server. The client and the server then sample random vectors per each linear layer from a finite ring, denoted by \mathbf{r}_i and \mathbf{s}_i respectively. The client encrypts its random vectors and sends them to the server. After obtaining $E(\mathbf{r}_i)$, the server computes $E(\mathbf{W}_i \cdot \mathbf{r}_i - \mathbf{s}_i)$ homomorphically and sends it back to the client. The client decrypts the ciphertext received from the server and stores the plaintext values. For each Non-

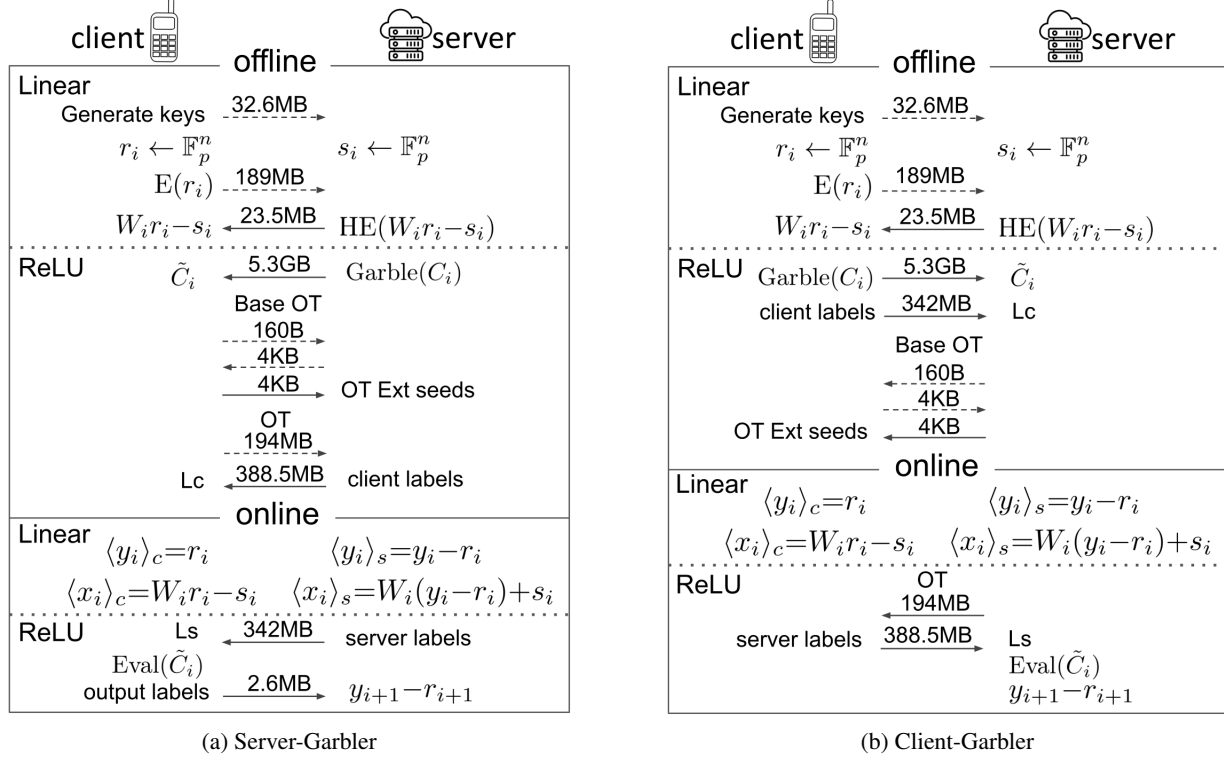


Figure 1. (a) The baseline “Server-Garbler” protocol used in prior work. Solid arrows in the offline phase of the protocol represent data that are stored by the recipient, while data communicated via dashed arrows can be discarded. (b) Proposed “Client-Garbler” protocol. Observe the significant reduction in offline storage on the client-side.

linear ReLU operation, the server constructs and garbles a circuit that implements $\text{ReLU}(\mathbf{x}_i) - \mathbf{r}_{i+1}$, where \mathbf{r}_{i+1} is the next layer randomness (provided by the client). The server sends the garbled circuits to the client and the two parties engage in the base OT protocol after which the client obtains labels corresponding to its inputs through the OT extension protocol. At the end of the offline phase, the server stores its random vectors \mathbf{s}_i and the garbled circuit input and output encodings, and the client stores its random vectors \mathbf{r}_i , garbled circuits, and the labels corresponding to its inputs. The communication and storage requirements for ResNet-32 inference on a single input from CIFAR-10 are shown in Figure 1(a). As depicted here, the largest storage requirement is 5.3 GB on the client due to garbled circuits.

Online Phase. The client’s input \mathbf{y}_1 is available in the online phase. The client computes $\mathbf{y}_1 - \mathbf{r}_1$ and sends it to the server. At the beginning of i th linear layer, the server holds $\mathbf{y}_i - \mathbf{r}_i$ and the client holds \mathbf{r}_i . The server computes its share of layer output as $\langle \mathbf{x}_i \rangle_s = \mathbf{W}_i(\mathbf{y}_i - \mathbf{r}_i) - \mathbf{s}_i$. The client holds $\langle \mathbf{x}_i \rangle_c = \mathbf{W}_i \cdot \mathbf{r}_i + \mathbf{s}_i$ from the offline phase, and the client and the server hold additive shares of $\mathbf{x}_i = \mathbf{W}_i \cdot \mathbf{y}_i$. To evaluate the ReLU layer, the server obtains the labels corresponding to its share of ReLU input $\langle \mathbf{x}_i \rangle_s$ and sends them to the client. The client now holds labels for the

server’s input, as well as labels for its inputs $\langle \mathbf{x}_i \rangle_c$ and \mathbf{r}_{i+1} , which were obtained during the offline phase along with the garbled circuits. The client evaluates the circuit and sends the output labels to the server who is then able to obtain $(\mathbf{y}_{i+1} - \mathbf{r}_{i+1})$. At this point, the client and server hold additive shares of \mathbf{y}_{i+1} and will similarly evaluate subsequent layers.

3 METHOD

In this section we first motivate our study by noting observations about the assumed baseline Server-Garbler protocol from existing work and how the storage and total performance costs limit its practical deployment. Next, we describe the proposed optimized Client-Garbler protocol and its benefits over the baseline solution.

3.1 Motivational Observations

Figure 2(a) and (b) respectively show the breakdown of computation and communication costs of the baseline PI protocol evaluated on a *single* inference, which is typical of prior work. The computation costs are dominated by HE, while the communication costs are dominated by GC.

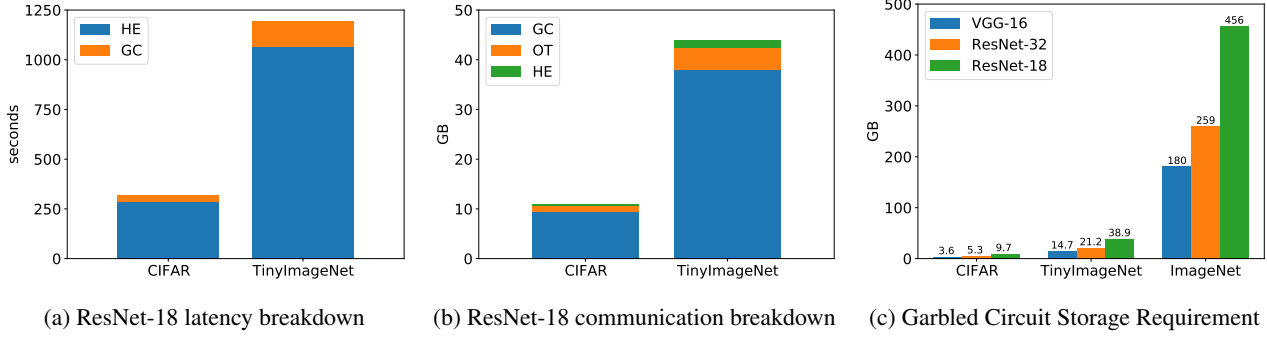


Figure 2. Latency and communication breakdown (Fig. a and Fig. b) for end-to-end *single image* encrypted inference on CIFAR-100 and TinyImageNet, and storage overhead (Fig. c) for the same on CIFAR-100, TinyImageNet, and ImageNet. Homomorphic evaluation of the linear layers dominates the compute latency, while Garbled Circuits dominate the communication between the server and client.

The key observation in DELPHI (Juvekar et al., 2018) was that HE computations involve only the server’s DNN model weights but not the client’s inputs. Therefore, assuming that the same model is used for multiple inferences, the computation costs of HE can be moved to input independent pre-compute/offline phase. Given that GC’s communication costs are always incurred offline, this means the online latency for a single inference can be reduced to roughly online GC computation costs and online OT communication costs, both of which are small. Table 2 shows that total online latency (including computation and communication latency) is more than 10× smaller than the offline latency.

Thus, as long as the client has sufficient downtime to perform pre-computations, it can achieve relatively fast inference results when requests arrive. For instance, ResNet-32 on CIFAR-100 has an online latency of 9.4s; while still far from real-time, a sub-10s latency is an encouraging result considering the strong security guarantee that PI provides.

However, the storage costs are shown in Figure 2(c) paint a different picture. The ResNet-32 model on CIFAR-100 incurs a 5.3GB storage cost, most of which is to store the garbled circuit on the client device assuming a standard server garbler protocol. (We stress here that although the garbled circuit is pre-computed, it cannot be used or amortized over multiple inferences. Each pre-computed garbled circuit can only be used for a single online inference and a new circuit must be pre-computed for the next inference.) Consider a client device with 8GB storage dedicated for PI. Such a device would only have the capacity to store a *single* pre-computation. This means that the client device would not have the opportunity to leverage any idle time between requests, due to either low request rates or variation in arrival times, to pre-compute and buffer computations, as there is simply no space to store them. Thus, as the request rate increases, large parts of the offline costs will be incurred online.

The picture is even bleaker for the TinyImageNet and ImageNet datasets. Depending on the network, the former requires between 14.7GB-38.9GB of largely client-side storage, a stretch for even high-end mobile phones, while the latter’s 180GB (or greater) storage costs are currently infeasible on most modern devices. Thus, private inference on ImageNet using existing Server-Garbler protocols cannot make use of pre-compute, moving the already large offline costs fully online.

3.2 Client-Garbler Protocol

In this section, we introduce our *Client-Garbler* protocol, which modifies the protocol described in Section 2.2 to alleviate the high storage requirements on the client. As discussed previously, this storage cost is largely due to the size of garbled circuits. We propose to *switch* the roles of the garbler and evaluator between the server and the client. Here the client plays the role of the garbler and the server plays the role of the evaluator. Hence, in our Client-Garbler protocol, the garbled circuits will be stored on the server, which we assume to have access to high-capacity storage. Our proposed Client-Garbler protocol is depicted in Figure 1(b). The linear layers (in offline and online phases) are processed as before.

During the offline phase for ReLU layers, the client garbles the circuits and sends them to the server along with the labels corresponding to its inputs (known in the offline phase). However, in this new protocol, the server can no longer acquire labels corresponding to its own inputs from the client in the offline phase since they depend on x , which is not known offline. The server must therefore wait to obtain these from the client *online* using OT while base OTs can however be performed offline. For ResNet-32 on CIFAR-100, the client’s offline storage costs in the client garbler protocol are only 23.5 MB while 5.3 GB is stored on the server for a ResNet-32 (Figure 1(b)).

Table 1. Network architecture and number of parameters, FLOPs, ReLUs, and accuracy (Acc(C100)) on CIFAR-100. Number of layers are in the order of (#Conv, #ReLU, #Avgpool, #FC) layers.

Model	#Layers	#Params	#FLOPs	#ReLUs	Acc(C100)
ResNet-32	(31, 31, 1, 1)	0.5M	68.9M	303.1K	67.03%
VGG-16	(13, 15, 5, 3)	34M	332.5M	284.7K	73.45%
ResNet-18	(17, 17, 1, 1)	11M	555.5M	557.1K	74.20%

* There are three additional 1×1 Conv layers in the skip connections which are not included here.

During the online phase, the server computes the linear layer and obtains its share of the output $\langle x_i \rangle_s$. The client and the server then engage in OT extension protocol and the server obtains the labels corresponding to its input. The server is now able to evaluate the GC and obtain the output, its share of the subsequent linear layer. The introduction of OT in the online phase can slightly increase online costs compared to Server-Garbler protocols. However, in return, we obtain massive reductions in client storage, and in end-to-end system evaluations, this results in a net performance benefit for the proposed Client-Garbler protocol. Still, when PI is evaluated from only the lens of a single inference, the server garbler protocol is slightly better. We note that both protocols have the same security because the security guarantees of GC do not depend on which party is the garbler.

4 EXPERIMENTAL RESULTS

Networks and Datasets: We performed experiments with ResNet models (He et al., 2016), ResNet-32 and ResNet-18, and VGG-16 (Simonyan & Zisserman, 2014) and we made the same architectural modifications to these networks as made in (Jha et al., 2021) and (Ghodsi et al., 2021). In particular, we remove the downsampling in earlier layers and replaced all the max-pooling operations with average-pooling as the latter is a linear operation and cheaper for PI. The layer, parameter, FLOPs, and ReLU counts for these networks are described in Table 1. We perform our experiments of CIFAR-100 (Krizhevsky et al., 2010) and TinyImageNet (Yao & Miller, 2015) dataset with 100 and 200 class labels, respectively. CIFAR-100 has images of spatial resolution 32×32 while TinyImageNet is more complex and has images of resolution 64×64 .

Experimental Setup: We develop a private inference simulator using the Simpy library to explore the full system effects of PI at scale (Meurer et al., 2017). We simulate both the conventional Server-Garbler and our proposed Client-Garbler protocol with a default bandwidth of 100 MB/sec. In our evaluations, we sweep client-side storage capacity from 8GB to 256GB and assume a 10TB storage on the server-side. We assume Poisson arrivals of inference requests at a given rate.

For a specified protocol, network, and dataset, we simulate

Table 2. Latency breakdown of Server-Garbler and Client-Garbler protocols for a single inference on CIFAR-100 (C100) and TinyImageNet (Tiny) datasets. The online latency of Client-Garbler is higher than Server-Garbler but the total latency of the former is lower than that of the latter.

Dataset	Model	Server-Garbler		Client-Garbler	
		Offline (s)	Online (s)	Offline (s)	Online (s)
C100	ResNet-32	115.2	9.4	109.1	11.9
	VGG-16	295.6	9.4	289.9	11.6
	ResNet-18	420.8	17.2	409.6	21.8
Tiny	ResNet-32	401.9	39.6	377.4	49.6
	VGG-16	814.7	34.2	792.2	43.4
	ResNet-18	1594.0	68.5	1549.1	86.9

24 hours of inference requests for a fixed arrival rate (assuming Poisson arrivals) and average inference latency over 100 simulation runs. Two processes are simulated concurrently: 1) the client and server check if enough storage is available to perform an offline phase in order to obtain precompute and Garbled Circuits and 2) the client and server engage in the online phase of either protocol if a private inference has been requested.

We model a single-client and single-server system where inference requests are queued and served in a First-In-First-Out manner. When an inference request moves out of the queue, the simulator checks the storage capacity for previously computed Garbled Circuits. If enough Garbled Circuits are available (for a single inference), the client and server begin executing the online phase of the configured protocol. If Garbled Circuits are not available, the client must wait for an offline phase to complete before performing the online phase.

We computed the latency, storage, and communication costs for the online and offline phase of both protocols using the DELPHI codebase. For all networks, we averaged these costs over 10 and 5 runs for CIFAR100- and TinyImageNet-like inputs, respectively. Finally, we input these costs into the simulator for both the offline and online phases.

4.1 Bottleneck 1 - GC Storage

Figure 3 compares the Server-Garbler and Client-Garbler protocol for the aforementioned networks and datasets. In particular, for the Server-Garbler protocol, we sweep both arrival rates and storage capacities. Client-side storage capacities range from 8 GB to 64 GB for CIFAR-100. For the proposed Client-Garbler protocol, we only simulate the smallest 8GB client-side capacity because this suffices to hold more than 300 pre-computes. The results are plotted in Figure 3a-c.

For all arrival rates, the proposed Client-Garbler protocol exhibits a lower mean inference latency when compared to

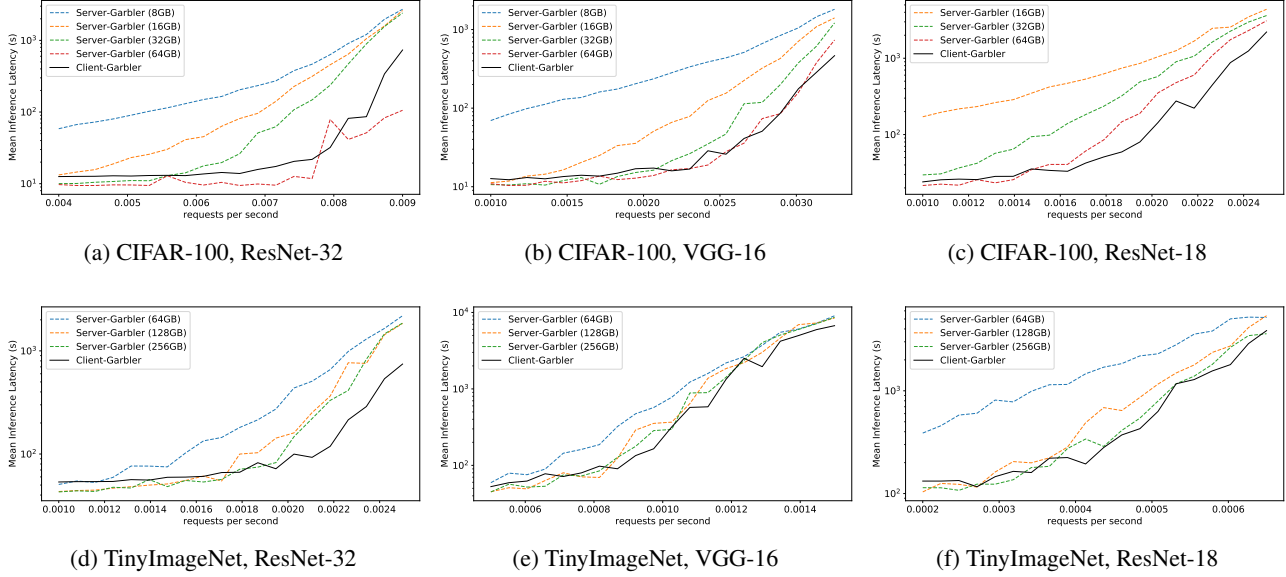


Figure 3. Comparison of the conventional Server-Garbler and our proposed Client-Garbler protocols for single image inference across varying arrival rates for CIFAR-100 (Fig. a-c) and TinyImageNet (Fig. d-f). For the Server-Garbler protocol, the high storage costs of Garbled Circuits prohibits the separation of an offline and online phase even for low to moderate arrival rates. On the other hand, the client-side storage requirements of the Client-Garbler protocol are much lower, mitigating this problem for low to medium arrival rates. At high arrival rates, HE compute latency dominates overall runtime for both protocols.

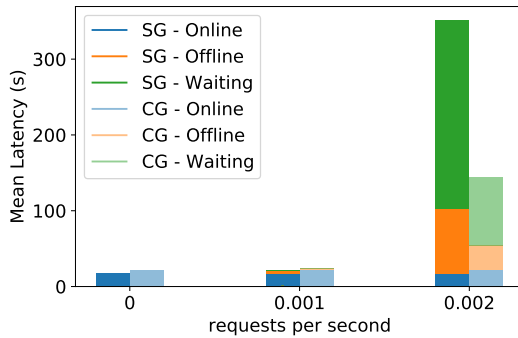


Figure 4. ResNet-18 latency breakdown for the conventional “Server-Garbler” (SG) and proposed “Client-Garbler” (CG) protocols on CIFAR-100 dataset.

the Server-Garbler protocol with 8 GB capacity (blue). This is because, with only 8 GB of storage for the Server-Garbler protocol, the client can only store at most one precompute for both ResNet-32 and VGG-16. We note that for ResNet-18, the client is unable to store even a single precompute with 8GB capacity as a single inference requires more than 9 GB of garbled circuits. Hence, for this network, we only plot results for 16 GB client-side storage and above.

For all networks, at 64 GB of client-side storage capacity (red), the mean inference latency for the Server-Garbler protocol is slightly lower than or similar to the Client-Garbler protocol, since enough capacity is now available to store

GC precomputes without saturating the queue. That is, even for CIFAR-100, the Server-Garbler needs up to 64 GB of storage to “catch up” to the Client-Garbler protocol which uses less than 8 GB storage. Every simulation begins with an empty storage capacity.

For the TinyImageNet dataset (see Figure 3d-f), we perform experiments with client-side storage capacity from 64 to 256 GB as the size of Garbled Circuits for a single inference ranges from 15 to 40 GB. Similar characteristics as to the CIFAR-100 experiments are observed for each network. We note a 4× reduction in mean PI latency at the arrival rate of 0.004 request/sec for ResNet-18 on TinyImageNet dataset.

4.2 Bottleneck 2 - Offline HE Latency

The Client-Garbler protocol enjoys the benefits of high capacity server-side storage for Garbled Circuits and precomputes, which can be observed at moderate arrival rates. However, at even higher arrival rates, the mean latency for the Client-Garbler protocol reaches on the order of hours for CIFAR-100. Figure 4 shows the breakdown of mean latency for a single inference request for three arrival rates for ResNet-18 on CIFAR-100. As the arrival rate increases, more cycles are spent waiting for offline precomputes to become available and previous inference requests to complete. As shown in Figure 2a, HE operations account for over 90% of latency during the offline phase. This issue is further aggravated by networks with higher FLOPs on com-

plex datasets such as ResNet-18 on TinyImageNet. Thus, the HE overhead cannot be mitigated at higher arrival rates and effectively becomes an online computation.

5 DISCUSSION AND RELATED WORK

5.1 Categorization of PI Methods

In this section, we discuss the efficacy of recently proposed PI techniques when considering their full-system effect with non-zero arrival requests rates. We categorize previous PI techniques into three categories based on how the FLOPs and ReLU savings affect the GC-cost per ReLU and HE-cost per FLOP depending on arrival rates: (1) low-arrival rate region, (2) moderate-arrival rate region, and (3) high-arrival rate region. We now describe the desirable optimization for each of these regions along with the applicability of PI optimization methods for each category.

Low-arrival rate region: As shown in Table 3, most of the previous PI methods are suitable only for low-arrival rates as they either substitute all the ReLUs with low-degree polynomials (e.g., CryptoNets, SecureML, Polyfit, CryptoDL, HCNN, Sisyphus, etc.) or reduce the number of non-linear operations by reducing the ReLU count of the network (e.g., DELPHI, CryptoNAS, SAFENets). However, in all these optimization strategies, the number of FLOPs (which affects HE costs) is usually disregarded. In fact, some of the ReLU-optimization increase the FLOPs count. For instance, CryptoNAS used neural architecture search and ReLU-balanced layers to find the ReLU-optimized networks while maximizing FLOPs per ReLU; under the assumption that ReLUs dominate PI runtime, this would maximize accuracy per ReLU, a desirable effect. This works very well for processing inferences in isolation. However, in a real-world setting where a system is expected to sustain a certain inference throughput, the increase in FLOPs worsens the HE cost, further straining the most costly performance bottleneck of the protocol.

Another common approach is to replace the PI-unfriendly ReLU activation function with polynomials, which can eliminate GC costs. It is worth noting that there is usually a significant accuracy penalty for this optimization (Garimella et al., 2021). Another recent work shows that to achieve reasonable accuracy on the ImageNet-1k dataset (Deng et al., 2009), a polynomial activation function must be of degree 29 needed (Lee et al., 2021). DELPHI and SAFENet (Lou et al., 2021) partially substituted some of a network’s ReLUs with low-degree polynomials assuming a baseline model is provided as input. While this will reduce GC costs, the FLOPs count remains the same across all the ReLU-optimized networks, which does not help with HE costs. On the other hand, CrypTFlow2 (Rathee et al., 2020) and Circa (Ghodsi et al., 2021) reduce the GC cost per ReLU computa-

tion, rather than replacing them. Thus, both the ReLU and FLOP counts remain the same. MiniONN (Liu et al., 2017), Gazelle (Juvekar et al., 2018), and AutoPrivacy (Lou et al., 2020a) neither reduce ReLU count nor the FLOPs count. AutoPrivacy does reduce the HE-cost per FLOP by automatically tuning the selection of HE-parameters on a layer-wise basis using the deep reinforcement learning technique.

Moderate-arrival rate region: In this region, we categorize the PI optimization methods with very low GC-cost (networks with only low-degree polynomials or very low ReLU count) and reduce HE-cost (either with reduced HE cost per FLOP or diminished FLOPs count). For instance, Faster-CryptoNets and HEMET have only low-degree polynomial activations and the former reduces the number of HE operations by introducing the sparsity in the network (using pruning and quantization) while the latter reduces the HE cost per FLOPs by reducing the multiplicative depth of the networks. However, the accuracy of Faster CryptoNets degrades substantially on CIFAR-10 and their efficacy on more complex datasets such as TinyImageNet needs to be evaluated. Similarly, HEMET showed the effectiveness on simpler networks such as SqueezeNet (Iandola et al., 2016) and InceptionNet (Szegedy et al., 2017).

On the other hand, DeepReDuce (a state-of-the-art in PI) drops the ReLUs by $5\times$ for ResNet-18 on CIFAR-100 and TinyImageNet without loss in accuracy and, and merges the consecutive linear (Conv) layers for FLOPs saving with $<1\%$ loss in accuracy. As a result, we believe this a promising direction of reducing both ReLU count (reducing GC costs) and FLOPs count (reducing HE costs).

High-arrival rate region: In this region, we consider the networks with (1) only polynomial activations, reduces HE-cost per FLOP and diminished FLOPs count (for instance Falcon), and (2) very-low ReLU count with reduced GC-cost per ReLU with diminished FLOPs count (e.g., DeepReDuce + Circa, Table 2 in (Ghodsi et al., 2021)). The accuracy of Falcon drops significantly for the CIFAR-10 dataset whereas Circa optimization on DeepReDuce works on complex datasets such as TinyImageNet. Altogether, with substantially reduced HE-cost along with low GC-cost, PI can be performed with a higher arrival rate. Additionally, we believe that efficient HE compilers (Dathathri et al., 2020; 2019; Cowan et al., 2021) can be used to further reduce the overall HE-cost and increase the maximal sustainable arrival rate.

In conclusion, low-arrival rate regions appeal to ReLU reduction strategies as Garbled Circuits are the main bottleneck in PI. However, in a real-world scenario which would include moderate to high arrival rates, HE costs move from the offline phase back to the online phase, and thus, it is necessary to optimize for both ReLU and FLOPs in order to sustain higher arrival rates.

Table 3. Comparison of the common PI methods from the viewpoint of their efficacy on full-system with non-zero arrival requests. Accuracy comparison are shown on MNIST (Deng, 2012), CIFAR-10 (C10), CIFAR-100 (C100), and TinyImageNet (Tiny) datasets. Number of \uparrow/\downarrow represents the extent of increase/decrease in the quantity compared to the baseline. Most of the previous PI methods performed optimization only for a single PI inference by considering only zero-arrival rate requests.

Arrival-rate	PI method	Online cost		Offline cost		Accuracy			
		#ReLU	$\frac{GC_{cost}}{ReLU}$	#FLOPs	$\frac{HE_{cost}}{FLOP}$	MNIST	C10	C100	Tiny
Low	CryptoNets (Gilad-Bachrach et al., 2016)	-	-	<i>Const</i>	<i>Const</i>	<i>Const</i>	-	-	-
	SecureML (Mohassel & Zhang, 2017)	-	-	<i>Const</i>	<i>Const</i>	\downarrow	-	-	-
	Polyfit (Chabanne et al., 2017)	-	-	<i>Const</i>	<i>Const</i>	\downarrow	-	-	-
	CryptoDL (Hesamifard et al., 2017)	-	-	<i>Const</i>	<i>Const</i>	<i>Const</i>	<i>Const</i>	-	-
	Lookup-Table (Thaine et al., 2019)	-	-	<i>Const</i>	<i>Const</i>	<i>Const</i>	-	-	-
	HCNN (Badawi et al., 2020)	-	-	<i>Const</i>	<i>Const</i>	<i>Const</i>	<i>Const</i>	-	-
	Sisyphus (Garimella et al., 2021)	-	-	<i>Const</i>	<i>Const</i>	<i>Const</i>	<i>Const</i>	$\downarrow\downarrow$	$\downarrow\downarrow\downarrow$
	MiniONN (Liu et al., 2017)	<i>Const</i>	<i>Const</i>	<i>Const</i>	<i>Const</i>	<i>Const</i>	<i>Const</i>	-	-
	GAZELLE (Juvekar et al., 2018)	<i>Const</i>	<i>Const</i>	<i>Const</i>	\downarrow	<i>Const</i>	<i>Const</i>	-	-
	DELPHI (Mishra et al., 2020)	\downarrow	<i>Const</i>	<i>Const</i>	<i>Const</i>	-	\downarrow	\downarrow	-
Moderate	CryptoNAS (Ghodsi et al., 2020)	$\downarrow\downarrow$	<i>Const</i>	$\uparrow\uparrow$	<i>Const</i>	-	<i>Const</i>	<i>Const</i>	-
	SAFENet (Lou et al., 2021)	$\downarrow\downarrow$	<i>Const</i>	<i>Const</i>	<i>Const</i>	-	\downarrow	\downarrow	-
	CrypTflow2 (Rathee et al., 2020)	<i>Const</i>	\downarrow	<i>Const</i>	<i>Const</i>	-	<i>Const</i>	<i>Const</i>	<i>Const</i> *
	Circa (Ghodsi et al., 2021)	<i>Const</i>	\downarrow	<i>Const</i>	<i>Const</i>	-	-	<i>Const</i>	<i>Const</i>
	AutoPrivacy (Lou et al., 2020a)	<i>Const</i>	<i>Const</i>	<i>Const</i>	\downarrow	-	<i>Const</i>	<i>Const</i>	-
High	F-CryptoNets (Chou et al., 2018)	-	-	\downarrow	<i>Const</i>	<i>Const</i>	$\downarrow\downarrow$	-	-
	HEMET (Lou & Jiang, 2021)	-	-	<i>Const</i>	\downarrow	-	<i>Const</i>	<i>Const</i>	-
High	DeepReDuce (Jha et al., 2021)	$\downarrow\downarrow$	<i>Const</i>	$\downarrow\downarrow^{**}$	<i>Const</i>	-	-	\downarrow	\downarrow
	Falcon (Lou et al., 2020b)	-	-	\downarrow	\downarrow	<i>Const</i>	\downarrow	-	-
	DeepReDuce + Circa	$\downarrow\downarrow$	\downarrow	$\downarrow\downarrow$	<i>Const</i>	-	-	\downarrow	\downarrow

* CrypTflow2 performed the PI on ImageNet-1k dataset with ResNet-50 and DenseNet-121

** DeepReDuce did not reduces the FLOPs for PI but showed the benefits of FLOPs reduction on plaintext (see Table 7 and Table 8 in (Jha et al., 2021))

6 RELATED WORK

Two-party PI methods which do not use HE Note that in the aforementioned categorization we do not consider the PI techniques which do not use HE for linear-layer computation. For instance, a few PI methods (Riazi et al., 2019; Samragh et al., 2021) use a Binary neural network (BNN) to reduce GC-cost by a huge margin; however, they showed their efficacy only on MNIST and CIFAR-10. It is well-known that BNN incurs the accuracy drop on complex datasets; even the state-of-the-art BNN suffers accuracy drop on ImageNet (Liu et al., 2020). DeepSecure (Rouhani et al., 2018), EzPC (Chandran et al., 2019), and Chameleon (Riazi et al., 2018) use GC for nonlinear operations and secret-sharing for linear operations. Similarly, CryptGPU (Tan et al., 2021) and CrypTen (Knott et al., 2021) use additive secret sharing for linear operations and binary secret sharing for nonlinear operation and rely on trusted-third party (TTP) for generating the beaver triples.

Private inference with more than two parties There has been a line of research work on three parties private inference. For instance, FALCON (Wagh et al., 2021), CrypTflow (Kumar et al., 2020), BLAZE (Patra & Suresh, 2020), SecureNN (Wagh et al., 2019), QuantizedNN (Dalskov et al., 2019), ASTRA (Chaudhari et al., 2019), ABY3 (Mohassel & Rindal, 2018), etc. Similarly, there has been four party

PI such as FLASH (Byali et al., 2020) and Trident (Rachuri & Suresh, 2019). However, the aforementioned PI methods have weak security model as they sacrificing security by making the assumption of a non-colluding third party.

7 CONCLUSION

In this paper, we investigate the end-to-end system characteristics of private inference. We find that most recently proposed PI protocols and optimizations focus only on reducing the online inference latency by moving compute-heavy HE cryptographic protocols to an offline phase. These online-only optimizations work well, but only for processing individual inferences, or when assuming an effective arrival rate of zero. We find that even for extremely low arrival rates, SOTA PI techniques are unable to endure the storage costs of garbled circuits. Consequently, clients are only able to process very few inferences (at very low arrival rates) at online-only performance before running out of storage and pre-computation before they have to incur both online and offline costs online, which degrades performance by an order of magnitude. To mitigate the storage issue, we proposed the Client-Garbler protocol to leverage the server’s high storage capacity. This optimization circumvents the storage bottleneck and enables low-latency inferences at low to moderate arrival rates, reducing the mean PI latency by

4× compared to the baseline approach. Finally, we note that recently proposed PI optimizations target online latency and ignore full system effects, thus limiting their true benefits.

ACKNOWLEDGEMENTS

This work was supported in part by the Applications Driving Architectures (ADA) Research Center, a JUMP Center co-sponsored by SRC and DARPA. This research was also developed with funding from the Defense Advanced Research Projects Agency (DARPA), under the Data Protection in Virtual Environments (DPRIVE) program, contract HR0011-21-9-0003. The views, opinions and/or findings expressed are those of the author and should not be interpreted as representing the official views or policies of the Department of Defense or the U.S. Government.

REFERENCES

Abadi, M., Chu, A., Goodfellow, I., McMahan, H. B., Mironov, I., Talwar, K., and Zhang, L. Deep learning with differential privacy. In *Proceedings of the 2016 ACM SIGSAC conference on computer and communications security*, pp. 308–318, 2016.

Anati, I., Gueron, S., Johnson, S. P., and Scarlata, V. R. Innovative technology for cpu based attestation and sealing, 2013.

Badawi, A. A., Chao, J., Lin, J., Mun, C. F., Sim, J. J., Tan, B. H. M., Nan, X., Aung, K. M. M., and Chandrasekhar, V. R. Towards the alexnet moment for homomorphic encryption: Hcnn, thefirst homomorphic cnn on encrypted data with gpus. *IEEE Transactions on Emerging Topics in Computing*, 2020.

Brakerski, Z. and Vaikuntanathan, V. Efficient fully homomorphic encryption from (standard) lwe. In *2011 IEEE 52nd Annual Symposium on Foundations of Computer Science*, pp. 97–106, 2011. doi: 10.1109/FOCS.2011.12.

Byali, M., Chaudhari, H., Patra, A., and Suresh, A. Flash: Fast and robust framework for privacy-preserving machine learning. *Proc. Priv. Enhancing Technol.*, 2020(2): 459–480, 2020.

Chabanne, H., de Wargny, A., Milgram, J., Morel, C., and Prouff, E. Privacy-preserving classification on deep neural network. *IACR Cryptol. ePrint Arch.*, 2017:35, 2017.

Chandran, N., Gupta, D., Rastogi, A., Sharma, R., and Tripathi, S. Ezpc: programmable and efficient secure two-party computation for machine learning. In *2019 IEEE European Symposium on Security and Privacy (EuroS&P)*, pp. 496–511. IEEE, 2019.

Chaudhari, H., Choudhury, A., Patra, A., and Suresh, A. Astra: high throughput 3pc over rings with application to secure prediction. In *Proceedings of the 2019 ACM SIGSAC Conference on Cloud Computing Security Workshop*, pp. 81–92, 2019.

Chou, E., Beal, J., Levy, D., Yeung, S., Haque, A., and Fei-Fei, L. Faster cryptonets: Leveraging sparsity for real-world encrypted inference. *arXiv preprint arXiv:1811.09953*, 2018.

Cowan, M., Dangwal, D., Alaghi, A., Trippel, C., Lee, V. T., and Reagen, B. Porcupine: a synthesizing compiler for vectorized homomorphic encryption. In *Proceedings of the 42nd ACM SIGPLAN International Conference on Programming Language Design and Implementation*, pp. 375–389, 2021.

Dalskov, A., Escudero, D., and Keller, M. Secure evaluation of quantized neural networks. *arXiv preprint arXiv:1910.12435*, 2019.

Dathathri, R., Saarikivi, O., Chen, H., Laine, K., Lauter, K., Maleki, S., Musuvathi, M., and Mytkowicz, T. Chet: an optimizing compiler for fully-homomorphic neural-network inferencing. In *Proceedings of the 40th ACM SIGPLAN Conference on Programming Language Design and Implementation*, pp. 142–156, 2019.

Dathathri, R., Kostova, B., Saarikivi, O., Dai, W., Laine, K., and Musuvathi, M. Eva: An encrypted vector arithmetic language and compiler for efficient homomorphic computation. In *Proceedings of the 41st ACM SIGPLAN Conference on Programming Language Design and Implementation*, pp. 546–561, 2020.

Deng, J., Dong, W., Socher, R., Li, L.-J., Li, K., and Fei-Fei, L. Imagenet: A large-scale hierarchical image database. In *2009 IEEE conference on computer vision and pattern recognition*, pp. 248–255. Ieee, 2009.

Deng, L. The mnist database of handwritten digit images for machine learning research [best of the web]. *IEEE Signal Processing Magazine*, 29(6):141–142, 2012.

Dwork, C. Differential privacy. In *International Colloquium on Automata, Languages, and Programming*, pp. 1–12. Springer, 2006.

Gallagher, M., Biernacki, L., Chen, S., Aweke, Z. B., Yitbarek, S. F., Aga, M. T., Harris, A., Xu, Z., Kasikci, B., Bertacco, V., et al. Morpheus: A vulnerability-tolerant secure architecture based on ensembles of moving target defenses with churn. In *Proceedings of the Twenty-Fourth International Conference on Architectural Support for Programming Languages and Operating Systems*, pp. 469–484, 2019.

Garimella, K., Jha, N. K., and Reagen, B. Sisyphus: A cautionary tale of using low-degree polynomial activations in privacy-preserving deep learning. In *ACM CCS Workshop on Private-preserving Machine Learning*, 2021.

Gentry, C. et al. *A fully homomorphic encryption scheme*. Stanford university, 2009.

Ghodsi, Z., Veldanda, A. K., Reagen, B., and Garg, S. CryptoNAS: Private inference on a relu budget. In *Advances in Neural Information Processing Systems*, volume 33, pp. 16961–16971, 2020.

Ghodsi, Z., Jha, N. K., Reagen, B., and Garg, S. Circa: Stochastic relus for private deep learning. In *Advances in Neural Information Processing Systems*, volume 34, 2021.

Gilad-Bachrach, R., Dowlin, N., Laine, K., Lauter, K., Naehrig, M., and Wernsing, J. Cryptonets: Applying neural networks to encrypted data with high throughput and accuracy. In *International Conference on Machine Learning*, pp. 201–210, 2016.

Hashemi, H., Wang, Y., and Annaram, M. DarKnight: An accelerated framework for privacy and integrity preserving deep learning using trusted hardware. In *54th Annual IEEE/ACM International Symposium on Microarchitecture*, pp. 212–224, 2021.

He, K., Zhang, X., Ren, S., and Sun, J. Deep residual learning for image recognition. In *Proceedings of the IEEE conference on computer vision and pattern recognition*, pp. 770–778, 2016.

Hesamifard, E., Takabi, H., and Ghasemi, M. CryptoDL: Deep neural networks over encrypted data. *arXiv preprint arXiv:1711.05189*, 2017.

Iandola, F. N., Han, S., Moskewicz, M. W., Ashraf, K., Dally, W. J., and Keutzer, K. SqueezeNet: Alexnet-level accuracy with 50x fewer parameters and; 0.5 mb model size. *arXiv preprint arXiv:1602.07360*, 2016.

Ishai, Y., Kilian, J., Nissim, K., and Petrank, E. Extending oblivious transfers efficiently. In *CRYPTO*, 2003.

Jha, N. K., Ghodsi, Z., Garg, S., and Reagen, B. DeepReduce: Relu reduction for fast private inference. In *International Conference on Machine Learning*, volume 139, pp. 4839–4849. PMLR, 2021.

Juvekar, C., Vaikuntanathan, V., and Chandrakasan, A. Gazelle: A low latency framework for secure neural network inference. In *27th USENIX Security Symposium (USENIX Security 18)*, pp. 1651–1669, 2018.

Knott, B., Venkataraman, S., Hannun, A., Sengupta, S., Ibrahim, M., and van der Maaten, L. CrypTen: Secure multi-party computation meets machine learning. *arXiv preprint arXiv:2109.00984*, 2021.

Krizhevsky, A., Nair, V., and Hinton, G. Cifar-10 (canadian institute for advanced research). URL <http://www.cs.toronto.edu/kriz/cifar.html>, 5, 2010.

Kumar, N., Rathee, M., Chandran, N., Gupta, D., Rastogi, A., and Sharma, R. Cryptflow: Secure tensorflow inference. In *2020 IEEE Symposium on Security and Privacy (SP)*, pp. 336–353. IEEE, 2020.

Lee, J., Lee, E., Lee, J.-W., Kim, Y., Kim, Y.-S., and No, J.-S. Precise approximation of convolutional neural networks for homomorphically encrypted data. *arXiv preprint arXiv:2105.10879*, 2021.

Liu, J., Juuti, M., Lu, Y., and Asokan, N. Oblivious neural network predictions via minionn transformations. In *Proceedings of the 2017 ACM SIGSAC Conference on Computer and Communications Security*, pp. 619–631, 2017.

Liu, Z., Shen, Z., Savvides, M., and Cheng, K.-T. Reactnet: Towards precise binary neural network with generalized activation functions. In *European Conference on Computer Vision*, pp. 143–159. Springer, 2020.

Lou, Q. and Jiang, L. Hemet: A homomorphic-encryption-friendly privacy-preserving mobile neural network architecture. volume 139, pp. 7102–7110. PMLR, 2021.

Lou, Q., Bian, S., and Jiang, L. Autoprivacy: Automated layer-wise parameter selection for secure neural network inference. In *Advances in Neural Information Processing Systems*, volume 33, pp. 8638–8647, 2020a.

Lou, Q., Lu, W.-j., Hong, C., and Jiang, L. Falcon: fast spectral inference on encrypted data. *Advances in Neural Information Processing Systems*, pp. 2364–2374, 2020b.

Lou, Q., Shen, Y., Jin, H., and Jiang, L. SAFENet: Asecure, accurate and fast neural network inference. *International Conference on Learning Representations*, 2021.

Meurer, A., Smith, C. P., Paprocki, M., Čertík, O., Kirpichev, S. B., Rocklin, M., Kumar, A., Ivanov, S., Moore, J. K., Singh, S., Rathnayake, T., Vig, S., Granger, B. E., Muller, R. P., Bonazzi, F., Gupta, H., Vats, S., Johansson, F., Pedregosa, F., Curry, M. J., Terrel, A. R., Roučka, v., Saboo, A., Fernando, I., Kulal, S., Cimrman, R., and Scopatz, A. Sympy: symbolic computing in python. *PeerJ Computer Science*, 3:e103, 2017.

Mishra, P., Lehmkuhl, R., Srinivasan, A., Zheng, W., and Popa, R. A. Delphi: A cryptographic inference service for

neural networks. In *29th USENIX Security Symposium (USENIX Security 20)*, 2020.

Mohassel, P. and Rindal, P. Aby3: A mixed protocol framework for machine learning. In *Proceedings of the 2018 ACM SIGSAC Conference on Computer and Communications Security*, pp. 35–52, 2018.

Mohassel, P. and Zhang, Y. SecureML: A system for scalable privacy-preserving machine learning. In *2017 IEEE Symposium on Security and Privacy (SP)*, pp. 19–38, 2017.

Patra, A. and Suresh, A. Blaze: blazing fast privacy-preserving machine learning. *arXiv preprint arXiv:2005.09042*, 2020.

Rabin, M. O. How to exchange secrets with oblivious transfer. *IACR Cryptol. ePrint Arch.*, 2005.

Rachuri, R. and Suresh, A. Trident: Efficient 4pc framework for privacy preserving machine learning. *arXiv preprint arXiv:1912.02631*, 2019.

Rathee, D., Rathee, M., Kumar, N., Chandran, N., Gupta, D., Rastogi, A., and Sharma, R. Cryptflow2: Practical 2-party secure inference. In *Proceedings of the 2020 ACM SIGSAC Conference on Computer and Communications Security*, pp. 325–342, 2020.

Riazi, M. S., Weinert, C., Tkachenko, O., Songhori, E. M., Schneider, T., and Koushanfar, F. Chameleon: A hybrid secure computation framework for machine learning applications. In *Proceedings of the 2018 on Asia Conference on Computer and Communications Security*, pp. 707–721. ACM, 2018.

Riazi, M. S., Samragh, M., Chen, H., Laine, K., Lauter, K., and Koushanfar, F. XONN: XNOR-based oblivious deep neural network inference. In *28th USENIX Security Symposium (USENIX Security 19)*, pp. 1501–1518, 2019.

Rivest, R. L., Adleman, L., Dertouzos, M. L., et al. On data banks and privacy homomorphisms. *Foundations of secure computation*, 4(11):169–180, 1978.

Rouhani, B. D., Riazi, M. S., and Koushanfar, F. Deepse-cure: Scalable provably-secure deep learning. In *Proceedings of the 55th Annual Design Automation Conference*, pp. 2, 2018.

Samragh, M., Hussain, S., Zhang, X., Huang, K., and Koushanfar, F. On the application of binary neural networks in oblivious inference. In *Proceedings of the IEEE/CVF Conference on Computer Vision and Pattern Recognition (CVPR) Workshops*, pp. 4630–4639, June 2021.

Shamir, A. How to share a secret. *Communications of the ACM*, 22(11):612–613, 1979.

Simonyan, K. and Zisserman, A. Very deep convolutional networks for large-scale image recognition. *arXiv preprint arXiv:1409.1556*, 2014.

Szegedy, C., Ioffe, S., Vanhoucke, V., and Alemi, A. A. Inception-v4, inception-resnet and the impact of residual connections on learning. In *Thirty-first AAAI conference on artificial intelligence*, 2017.

Tan, S., Knott, B., Tian, Y., and Wu, D. J. CryptGPU: Fast privacy-preserving machine learning on the gpu. In *2021 IEEE Symposium on Security and Privacy (SP)*, pp. 1021–1038, 2021.

Thaine, P., Gorbunov, S., and Penn, G. Efficient evaluation of activation functions over encrypted data. In *2019 IEEE Security and Privacy Workshops (SPW)*, pp. 57–63. IEEE, 2019.

Tramer, F. and Boneh, D. Slalom: Fast, verifiable and private execution of neural networks in trusted hardware. *arXiv preprint arXiv:1806.03287*, 2018.

Van Bulck, J., Minkin, M., Weisse, O., Genkin, D., Kasikci, B., Piessens, F., Silberstein, M., Wenisch, T. F., Yarom, Y., and Strackx, R. Foreshadow: Extracting the keys to the intel {SGX} kingdom with transient out-of-order execution. In *27th {USENIX} Security Symposium ({USENIX} Security 18)*, pp. 991–1008, 2018.

Wagh, S., Gupta, D., and Chandran, N. Securenn: 3-party secure computation for neural network training. *Proc. Priv. Enhancing Technol.*, 2019(3):26–49, 2019.

Wagh, S., Tople, S., Benhamouda, F., Kushilevitz, E., Mittal, P., and Rabin, T. FALCON: Honest-Majority Maliciously Secure Framework for Private Deep Learning. 2021.

Wood, A., Altman, M., Bembenek, A., Bun, M., Gaboardi, M., Honaker, J., Nissim, K., O’Brien, D. R., Steinke, T., and Vadhan, S. Differential privacy: A primer for a non-technical audience. *Vand. J. Ent. & Tech. L.*, 21:209, 2018.

Yao, A. C.-C. How to generate and exchange secrets. In *27th Annual Symposium on Foundations of Computer Science (sfcs 1986)*, pp. 162–167, 1986.

Yao, L. and Miller, J. Tiny imagenet classification with convolutional neural networks. *CS 231N*, 2(5):8, 2015.